


Continuous-variable Clauser-Horne Bell-type inequality: A tool to unearth the nonlocality of continuous-variable quantum-optical systems

Chandan Kumar,^{*} Gaurav Saxena[†] and Arvind[‡]

Department of Physical Sciences, Indian Institute of Science Education and Research Mohali, Sector 81 SAS Nagar, Punjab 140306, India

 (Received 22 August 2020; revised 13 April 2021; accepted 13 April 2021; published 28 April 2021)

We consider a continuous-variable Clauser-Horne Bell-type inequality to study nonlocality in four-mode continuous-variable systems, which goes beyond two-photon states and can be applied to mixed as well as to states with fluctuating photon number. We apply the inequality to a wide variety of states such as pure and mixed Gaussian states (including squeezed thermal states) and non-Gaussian states. We consider beam splitters as a model for leakage and show that the inequality is able to detect nonlocality of noisy Gaussian states as well. Finally, we investigate nonlocality in pair-coherent states and entangled coherent states, which are prominent examples of nonclassical, non-Gaussian states.

DOI: [10.1103/PhysRevA.103.042224](https://doi.org/10.1103/PhysRevA.103.042224)

I. INTRODUCTION

In 1935, Albert Einstein, Boris Podolsky, and Nathan Rosen in their famous EPR paper alluded to the possibility of the incompleteness of quantum mechanics [1]. Bell's seminal work of 1964 showed that attempts to complete quantum mechanics within a local framework is impossible [2]. The important concepts of entanglement and nonlocality which arose from this context have occupied the imagination of physicists ever since and now play a major role in the area of quantum information [3,4]. Violation of Bell's inequality by the predictions of quantum mechanics is an indication of quantum nonlocality and is the strongest form of all quantum correlations [5]. The relationship between entanglement, nonlocality, Bell violation, and the classical-quantum divide can be complicated. While results of spacelike separated measurements on distant parties with classical correlations always satisfy Bell inequalities, such measurements on pure entangled states always violate Bell inequalities. However, there exist mixed entangled states which do not violate any Bell inequalities and there have been efforts to establish a quantitative relation between these two concepts [6–8]. There also exist nonseparable states with nonseparable classical correlations between two different degrees of freedom in the same classical beam of light [9,10]. Such states have been shown to violate Bell's inequality [11–15]. It is not always necessary for a state to have entanglement for exhibiting nonlocality [16,17]. As we shall see, the continuous-variable Clauser-Horne (CV-CH) Bell-type inequality that we consider detects

intermode quantum correlations and is not violated if the state is separable.

In the original EPR paper [1], states entangled in a continuous degree of freedom (position) were considered. However, most research in nonlocality has been conducted on discrete variable systems which involve the famous form of Bell inequality known as the CHSH inequality [18,19]. Nonlocality is useful in a wide variety of applications such as quantum communication and secure quantum key distribution [20–24]. While the CHSH inequality is sufficient for bipartite two-level systems [5,18,19,25], there have been efforts in the direction of generalizing Bell-CHSH inequality for multipartite systems [26–32].

Formulating Bell's inequalities for continuous variable (CV) systems is important as it allows us to connect with quantum-optical systems and helps us in investigating the notion of quantumness in a variety of new situations. Efforts have been made to construct Bell-type inequalities for CV systems with different number of modes [33–38]. Specifically a generalization of the CHSH inequality for CV systems was carried out using measurement operators having two outcomes [33–35,39]. In this formulation, modes were considered as entities, and the analysis was not restricted to states with a fixed number of photons. While several studies have been performed on pinning down nonlocality via Bell-type inequalities in various states of the CV systems [40–45], the formulation of universal Bell-type inequalities for CV systems still remains an open problem.

In quantum optics, if diagonal coherent state representation function corresponding to a quantum state is positive and no more singular than a delta function, the state is classified as classical, otherwise it is considered to be nonclassical [46,47]. Classical states can be simulated by ensembles of solutions of Maxwell equations, while nonclassical states have intrinsic quantum properties. The classical or nonclassical status of a state is unaffected by the action of passive optical elements which conserve the total photon number. On the other hand, quantum nonlocality captured via Bell-type inequalities

^{*}chandankumar@iisermohali.ac.in

[†]gaurav.saxena1@ucalgary.ca; Present Address: Department of Physics and Astronomy and Institute for Quantum Science and Technology (IQST), University of Calgary, Calgary T2N1N4, Alberta, Canada.

[‡]arvind@iisermohali.ac.in; Also at Punjabi University Patiala, Punjab 147002, India.

is a consequence of quantum entanglement, which arises in composite systems where intrinsically quantum correlations exist. The connection between these two quantum features is therefore very interesting and profound [48–50]. In fact there is a possibility of converting nonclassicality into entanglement or discord via passive optics [51–57]. The notions of classicality based on locality and optical considerations are called C-classicality and P-classicality, respectively [50]. In our study, we demonstrate how CV-CH Bell-type inequalities provide an experimentally testable connection between these two types of nonclassicalities.

In this work, we apply the CV-CH Bell-type inequality [33] to several situations in order to demonstrate its usefulness. First, we analyze the inequality for different two-photon states, and then consider general pure Gaussian states. Note that Gaussian measurements cannot be used to detect nonlocality of input Gaussian states [18]. However, we have used non-Gaussian measurements (on-off detectors) in our setup and hence, our setup can detect nonlocality in Gaussian as well as non-Gaussian states [58–60]. The optical circuits that we consider convert nonclassical squeezing into entanglement, which leads to the violation of the inequality. The analysis of mixed states with noise is carried out for thermal Gaussian states and for the case where dissipation leading to loss of photons is modeled by using beam splitters. Nonlocality vanishes in the case of thermal states once the temperature reaches a certain value, while nonlocality remains preserved for all nonzero transmittance values for the photon loss case modeled via beam splitters. Moving beyond the class of Gaussian states, we analyze pair coherent states and “entangled coherent states,” which are non-Gaussian nonclassical states and find that they are indeed nonlocal and violate the CV-CH Bell-type inequality.

This paper is organized as follows. In Sec. II, we briefly discuss the CV-CH Bell violation setup that we use in this work. Section III A discusses nonlocality in two-photon states, while Sec. III B discusses nonlocality in four-mode general Gaussian states. Section III C considers non-Gaussian states. Section IV provides a summary of our results and future directions. In the Appendix we describe details of phase space description of the CV systems which is used in our work.

II. THE CV-CH BELL VIOLATION SCENARIO

In this section, we describe the setup which we consider for the violation of Bell type inequalities. We consider a four-mode optical system where modes are labeled by two wave vectors described by \mathbf{k} and \mathbf{k}' and two polarizations are possible for each direction as depicted in Fig. 1. We label the polarization basis by \hat{x} and \hat{y} and by \hat{x}' and \hat{y}' for the propagation directions \mathbf{k} and \mathbf{k}' , respectively. Quantum mechanically each mode is described by an annihilation operator; annihilation operators \hat{a}_1 and \hat{a}_2 represent the two polarization modes for direction \mathbf{k} , while annihilation operators \hat{a}_3 and \hat{a}_4 correspond to the polarization modes for the direction \mathbf{k}' . We first prepare the state by applying compact passive transformations $U(4)$ consisting of beam splitters, phase shifters, and wave plates on a nonclassical and separable state. Subsequently, the photons in each propagation direction are filtered by a polarizer placed in a particular direction to select pho-

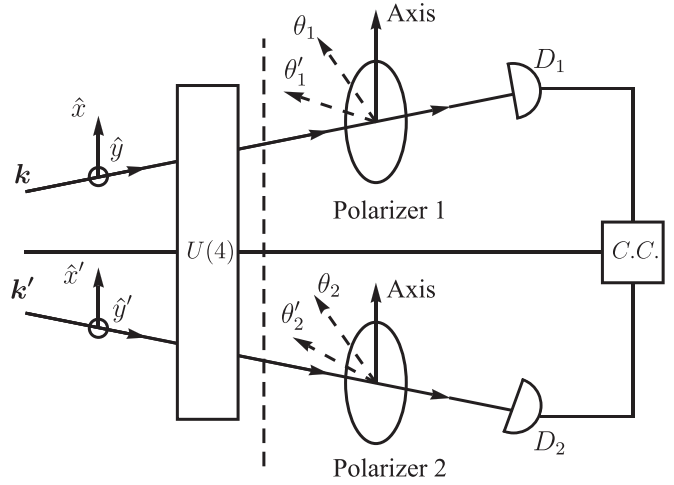


FIG. 1. Setup to study Bell inequality violation for states of a four-mode radiation field.

tions with a certain linear polarization. After this selection, the coincidence counts are recorded using an on-off detector, which performs coarse-grained measurements in the sense it distinguishes “light” from “no-light.”

We define four dichotomous Hermitian operators which enable us to evaluate coincidence count rates and can be used in the CHSH inequality as follows:

$$\begin{aligned} \hat{A} &= (I_{2 \times 2} - |00\rangle\langle 00|)_{\mathbf{k}}, \\ \hat{B} &= (I_{2 \times 2} - |00\rangle\langle 00|)_{\mathbf{k}'}, \\ \hat{A}_{\theta_1} &= (I_{\theta_1} - |0\rangle_{\theta_1}\langle 0|)I_{\theta_1 + \frac{\pi}{2}}, \\ \hat{B}_{\theta_2} &= (I_{\theta_2} - |0\rangle_{\theta_2}\langle 0|)I_{\theta_2 + \frac{\pi}{2}}, \end{aligned} \quad (1)$$

where the subscripts θ_1 and θ_2 are the directions of the polarizers and A and B are used to represent operators in the propagation directions \mathbf{k} and \mathbf{k}' , respectively. The operators \hat{A} , \hat{A}_{θ_1} , \hat{B} , and \hat{B}_{θ_2} incorporate the quantum mechanical action of the polarizers and are convenient for mathematical calculations of the averages. Further, the operator I_{θ_1} represents a unit operator for the single mode system with wave vector \mathbf{k} and polarization θ_1 , whereas the operator $I_{\theta_1 + \frac{\pi}{2}}$ represents a unit operator for the orthogonal polarization. The operators I_{θ_2} and $I_{\theta_2 + \frac{\pi}{2}}$ can be defined in a similar way. The operators \hat{A} and \hat{A}_{θ_1} act on the Hilbert space of modes \hat{a}_1 and \hat{a}_2 . The expectation value of \hat{A} is the probability of finding at least one photon with no polarizer placed in the path, while the expectation value of \hat{A}_{θ_1} is the probability of finding at least one photon after a polarizer has been placed in the path. The operators \hat{B} and \hat{B}_{θ_2} play a similar role for the modes \hat{a}_3 and \hat{a}_4 . Detectors $D1$ and $D2$ are the usual on-off detectors and are represented by the POVM operators $\{|0\rangle\langle 0|, I - |0\rangle\langle 0|\}$. The measurement performed by the on-off detectors is a non-Gaussian one as the POVM element $I - |0\rangle\langle 0|$ is a non-Gaussian operator.

We now define four different types of coincidence count rates based on different settings of the two polarizers as follows:

- (i) $P(\theta_1, \theta_2) = \langle \hat{A}_{\theta_1} \hat{B}_{\theta_2} \rangle :=$ The first polarizer at θ_1 and the second one at θ_2 with respect to their respective x axes.

(ii) $P(\theta_1, \theta_2) = \langle \hat{A}_{\theta_1} \hat{B}_{\theta_2} \rangle :=$ The first polarizer at θ_1 and the second one removed.

(iii) $P(\theta_1, \theta_2) = \langle \hat{A}_{\theta_1} \hat{B}_{\theta_2} \rangle :=$ The first polarizer removed and the second one at θ_2 .

(iv) $P(\theta_1, \theta_2) = \langle \hat{A}_{\theta_1} \hat{B}_{\theta_2} \rangle :=$ Both the polarizers removed from the setup.

If the quantum state of the four-mode field is known, then the above coincidence count rates can be readily evaluated.

If we assume that there is local hidden variable model (LHVM) which can explain the outcomes of measurement of operators given in Eq. (1), the coincident count rates have to satisfy following inequality [61]:

$$-P(\theta_1, \theta_2) \leq P(\theta_1, \theta_2) - P(\theta_1, \theta_2') + P(\theta_1', \theta_2) + P(\theta_1', \theta_2') - P(\theta_1', \theta_2) - P(\theta_1, \theta_2) \leq 0. \quad (2)$$

This is the state-independent Bell-type inequality valid for general radiation states and its violation (using quantum theory) by a given quantum state proves that the state has nonlocal quantum correlations that cannot be accommodated in realist hidden variable models based on locality. It is worth emphasizing that we have used operators defined on the four-mode field and did not imagine the photon as a single particle moving along a trajectory. In fact the states that we encounter may not even have a fixed number of photons. More details regarding this inequality is available in [33].

III. NONLOCALITY USING CV-CH BELL-TYPE INEQUALITY

In this section, we present our main results where we apply the CV-CH Bell-type inequality to different four-mode states of the optical field. We begin with two-photon states, and then consider a variety of four-mode Gaussian and non-Gaussian states.

A. Two-photon states

We consider two examples of two-photon states which are generated by applying compact passive transformations comprising beam splitters, phase shifters, and wave plates. An arbitrary passive transformation acting on our four-mode system with two spatial modes and each mode having two distinct polarizations can be written as [see Eq. (A23) of the Appendix for more details]

$$U = \begin{pmatrix} U_1 & 0 \\ 0 & U_2 \end{pmatrix} \underbrace{\begin{pmatrix} C & S \\ -S & C \end{pmatrix}}_D \begin{pmatrix} V_1^T & 0 \\ 0 & V_2^T \end{pmatrix}. \quad (3)$$

To generate the first state $|\psi_1\rangle$, we apply the U transformation (3), with

$$U_1 = U_2 = \frac{1}{\sqrt{2}} \begin{pmatrix} 1 & -1 \\ 1 & 1 \end{pmatrix}, \quad V_1 = V_2 = \mathbb{1}_2, \quad D = \mathbb{1}_4, \quad (4)$$

on a nonclassical and separable state:

$$\begin{aligned} |0\rangle_1 |1\rangle_2 |0\rangle_3 |1\rangle_4 &\xrightarrow{U(U_1) \otimes U(U_2)} \frac{1}{2} (|01\rangle - |10\rangle)_{12} (|01\rangle - |10\rangle)_{34} \\ |\psi_1\rangle &= \frac{1}{2} (|1\rangle_1 |0\rangle_2 |1\rangle_3 |0\rangle_4 - |1\rangle_1 |0\rangle_2 |0\rangle_3 |1\rangle_4 \\ &\quad - |0\rangle_1 |1\rangle_2 |1\rangle_3 |0\rangle_4 + |0\rangle_1 |1\rangle_2 |0\rangle_3 |1\rangle_4), \end{aligned} \quad (5)$$

where $U(U_1)$ and $U(U_2)$ belong to the infinite dimensional unitary (metaplectic) representation of U_1 and U_2 and act on the modes 1 & 2 (\mathbf{k}) and modes 3 & 4 (\mathbf{k}'), respectively. It should be noted that the initial state before the passive transformation is separable and nonclassical; however, the final state obtained after the passive transformation is clearly entangled. The role of passive transformations in the generation of quantum correlations have been discussed in the Appendix.

Similarly, the second state $|\psi_2\rangle$ is generated by applying the compact unitary transformation (3) with

$$C = -S = (1/\sqrt{2})\mathbb{1}_2, \quad U_1 = U_2 = V_1 = V_2 = \mathbb{1}_2, \quad (6)$$

on a nonclassical and separable state:

$$\begin{aligned} |0\rangle_1 |0\rangle_2 |1\rangle_3 |1\rangle_4 &\xrightarrow{U(D)} \frac{1}{2} (|01\rangle - |10\rangle)_{13} (|01\rangle - |10\rangle)_{24} \\ |\psi_2\rangle &= \frac{1}{2} (|1\rangle_1 |1\rangle_2 |0\rangle_3 |0\rangle_4 - |1\rangle_1 |0\rangle_2 |0\rangle_3 |1\rangle_4 \\ &\quad - |0\rangle_1 |1\rangle_2 |1\rangle_3 |0\rangle_4 + |0\rangle_1 |0\rangle_2 |1\rangle_3 |1\rangle_4). \end{aligned} \quad (7)$$

This transformation mixes the pair of modes 1 & 2 (\mathbf{k}) with the pair of modes 3 & 4 (\mathbf{k}').

Explicit calculation shows that $|\psi_1\rangle$ does not violate the CV-CH Bell-type inequality (2) for any value of $\theta_1, \theta_2, \theta_1', \theta_2'$; however, the state $|\psi_2\rangle$ does violate the inequality for some values of $\theta_1, \theta_2, \theta_1', \theta_2'$. In the first case since there is no entanglement between modes belonging to two different directions, all the correlation functions factorize, for example,

$$P(\theta_1, \theta_2) = \langle \hat{A}_1(\theta_1) \hat{A}_2(\theta_2) \rangle = \langle \hat{A}_1(\theta_1) \rangle \langle \hat{A}_2(\theta_2) \rangle. \quad (8)$$

Therefore, the CV-CH Bell-type inequality is obeyed. However, in state $|\psi_2\rangle$, entanglement is present in modes 1–3 and modes 2–4. Here, unlike Eq. (8), the correlation functions, for instance, $\langle \hat{A}_1(\theta_1) \hat{A}_2(\theta_2) \rangle \neq \langle \hat{A}_1(\theta_1) \rangle \langle \hat{A}_2(\theta_2) \rangle$, do not factorize and this results in the violation of the Bell-type inequality. Thus, CV-CH Bell-type inequality (2) is designed to detect nonlocality if entanglement exists between either of the modes along different directions.

B. Four-mode Gaussian states

In this section we consider various situations involving four-mode Gaussian states. We consider pure as well mixed cases and also consider leakage modeled by beam splitters.

1. Generic four-mode Gaussians

To produce a generic four-mode Gaussian state, we start with a four-mode vacuum state or a thermal state and then apply squeezing transformations on individual modes. The first and second modes are squeezed by an equal amount u and the third and fourth modes are squeezed by an equal amount v . The combined symplectic transformation corresponding to the squeezing transformations is denoted by $S(u, v)$. The mathematical expression for $S(u, v)$ can be readily obtained

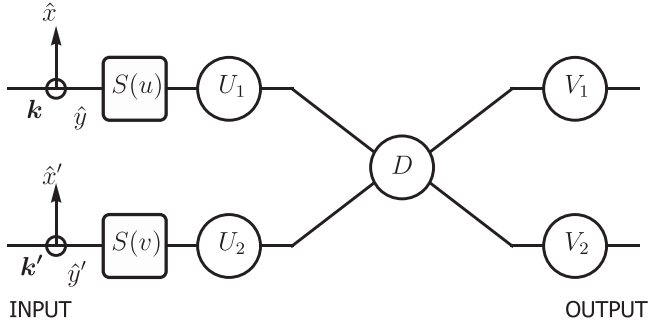


FIG. 2. Schematic to generate a four-mode entangled state. Here $S(u)$ and $S(v)$ represent squeezing transformations. Further, U_1 , U_2 , V_1 , and V_2 represent transformations that can be generated by combinations of quarter- and half-wave plates and phase shifters, while D represents transformations that can be generated using beam splitters and quarter- and half-wave plates. The first part of the circuit generates nonclassicality by squeezing the individual modes and the passive operations comprising beam splitter, phase shifters, and quarter- and half-wave plates convert the nonclassicality into entanglement. Classical $\xrightarrow{\text{Squeezing}}$ Nonclassical $\xrightarrow{\text{Passive operations}}$ Entangled.

using Eq. (A15) given in the Appendix as follows.

$$S(u, v) = \begin{pmatrix} q_1 & q_2 & q_3 & q_4 & p_1 & p_2 & p_3 & p_4 \\ e^{-u} & 0 & 0 & 0 & 0 & 0 & 0 & 0 \\ 0 & e^{-u} & 0 & 0 & 0 & 0 & 0 & 0 \\ 0 & 0 & e^{-v} & 0 & 0 & 0 & 0 & 0 \\ 0 & 0 & 0 & e^{-v} & 0 & 0 & 0 & 0 \\ \hline 0 & 0 & 0 & 0 & e^u & 0 & 0 & 0 \\ 0 & 0 & 0 & 0 & 0 & e^u & 0 & 0 \\ 0 & 0 & 0 & 0 & 0 & 0 & e^v & 0 \\ 0 & 0 & 0 & 0 & 0 & 0 & 0 & e^v \end{pmatrix} \begin{matrix} q_1 \\ q_2 \\ q_3 \\ q_4 \\ p_1 \\ p_2 \\ p_3 \\ p_4 \end{matrix} \quad (9)$$

Subsequently, the state is passed through a particular setting of beam splitter, phase shifters, and quarter- and half-wave plates producing an entangled state as illustrated in Fig. 2. We consider the passive transformation which generates the maximum amount of entanglement when acting on a system with four modes. The corresponding matrix acting on the annihilation operators $(\hat{a}_1, \hat{a}_2, \hat{a}_3, \hat{a}_4)^T$ is given by

$$U = \frac{1}{2} \begin{pmatrix} 1 & -1 & -1 & 1 \\ 1 & 1 & -1 & -1 \\ 1 & -1 & 1 & -1 \\ 1 & 1 & 1 & 1 \end{pmatrix}. \quad (10)$$

This can be decomposed in terms of submatrices using the form given in Eq. (3) as follows:

$$U_1 = -U_2 = \frac{1}{\sqrt{2}} \begin{pmatrix} 1 & 1 \\ -1 & 1 \end{pmatrix}, \quad V_1 = -V_2 = \begin{pmatrix} 0 & 1 \\ -1 & 0 \end{pmatrix},$$

$$\text{and } C = S = \frac{1}{\sqrt{2}} \begin{pmatrix} 1 & 0 \\ 0 & 1 \end{pmatrix}. \quad (11)$$

Here U_1 , U_2 , V_1 , and V_2 represent transformations that can be generated by combinations of wave plates and phase shifters, while $D = \begin{pmatrix} C & S \\ -S & C \end{pmatrix}$ can be generated using beam splitters and wave plates.

The corresponding passive transformation acting on the Hermitian quadrature operators $\hat{\xi}$ can be written as follows using Eq. (A11) given in the Appendix.

$$K = \frac{1}{2} \begin{pmatrix} q_1 & q_2 & q_3 & q_4 & p_1 & p_2 & p_3 & p_4 \\ \hline 1 & -1 & -1 & 1 & 0 & 0 & 0 & 0 \\ 1 & 1 & -1 & -1 & 0 & 0 & 0 & 0 \\ 1 & -1 & 1 & -1 & 0 & 0 & 0 & 0 \\ 1 & 1 & 1 & 1 & 0 & 0 & 0 & 0 \\ \hline 0 & 0 & 0 & 0 & 1 & -1 & -1 & 1 \\ 0 & 0 & 0 & 0 & 1 & 1 & -1 & -1 \\ 0 & 0 & 0 & 0 & 1 & -1 & 1 & -1 \\ 0 & 0 & 0 & 0 & 1 & 1 & 1 & 1 \end{pmatrix} \begin{matrix} q_1 \\ q_2 \\ q_3 \\ q_4 \\ p_1 \\ p_2 \\ p_3 \\ p_4 \end{matrix} \quad (12)$$

We can write the covariance matrix of the final state generated by the symplectic transformation $S = KS(u, v)$ acting on the thermal state as

$$V = KS(u, v)V_0S(u, v)^TK^T, \quad (13)$$

where

$$V_0 = \frac{1}{2\kappa} \mathbb{1}_{8 \times 8}, \quad \text{where } \kappa = \tanh\left(\frac{\hbar\omega}{2kT}\right) \text{ \& } 0 \leq \kappa \leq 1, \quad (14)$$

is the four-mode thermal state. Thus, $G = (1/2)V^{-1}$ can be expressed as

$$G = KS(u, v)^{-1}G_0S(u, v)^{-1}K^{-1}, \quad (15)$$

where $G_0 = \kappa \mathbb{1}_{8 \times 8}$. This G matrix enables us to write the Wigner function for any given state using Eq. (A28) given in the Appendix. To analyze the nonlocality of the four-mode generic Gaussian state, we consider the average of the Bell operator,

$$\begin{aligned} f(\theta_1, \theta_2, \theta'_1, \theta'_2) &= P(\theta_1, \theta_2)_{\text{qm}}^{\text{Gauss}} - P(\theta_1, \theta'_2)_{\text{qm}}^{\text{Gauss}} \\ &\quad + P(\theta'_1, \theta_2)_{\text{qm}}^{\text{Gauss}} + P(\theta'_1, \theta'_2)_{\text{qm}}^{\text{Gauss}} \\ &\quad - P(\theta'_1, \theta_2)_{\text{qm}}^{\text{Gauss}} - P(\theta_1, \theta'_2)_{\text{qm}}^{\text{Gauss}}. \end{aligned} \quad (16)$$

We show the calculation for one of the correlation functions involved above:

$$\begin{aligned} P(\theta_1, \theta_2)_{\text{qm}}^{\text{Gauss}} &= 1 - \text{Tr}(\rho|0\rangle_{\theta_1\theta_1}\langle 0|) - \text{Tr}(\rho|0\rangle_{\theta_2\theta_2}\langle 0|) \\ &\quad + \text{Tr}(\rho|0\rangle_{\theta_1\theta_1}\langle 0||0\rangle_{\theta_2\theta_2}\langle 0|). \end{aligned} \quad (17)$$

The evaluation of the second term of the above expression using Eq. (A29) given in Appendix A in the phase space picture is shown below, while the other terms can be calculated in a similar way:

$$\begin{aligned} \text{Tr}(\rho|0\rangle_{\theta_1\theta_1}\langle 0|) &= 2\pi \int W(U(\theta_1, 0)\xi)W_0(q_1, p_1)d\xi \\ &= 2\sqrt{\text{Det}(G)}\sqrt{\text{Det}[U(\theta_1, 0)^T G U(\theta_1, 0) + e_{11} + e_{55}]^{-1}}, \end{aligned} \quad (18a)$$

$$(18b)$$

where $U(\theta_1, \theta_2) = R(\theta_1) \oplus R(\theta_2) \oplus R(\theta_1) \oplus R(\theta_2)$ with

$$R(\theta) = \begin{pmatrix} \cos \theta & -\sin \theta \\ \sin \theta & \cos \theta \end{pmatrix}, \quad (19)$$

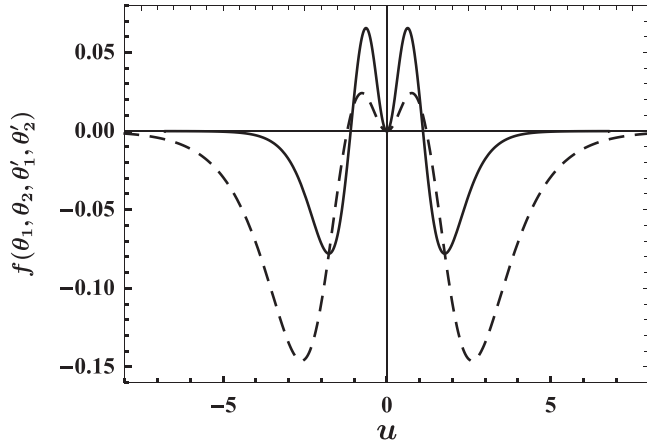


FIG. 3. Average of Bell operator as a function of squeezing parameter u for the four-mode pure squeezed vacuum state. Different angles are fixed as $\theta_1 = 1.32$, $\theta_2 = 0.93$, $\theta'_1 = 3.66$, $\theta'_2 = 3.32$. Thick solid line represents the case $v = -u$ corresponding to the state $|\text{TMSV}\rangle_{13}|\text{TMSV}\rangle_{24}$ showing violation of the CV-CH Bell-type inequality. Dashed line corresponds to $v = 0$, which also violates the inequality although to a less extent.

is the rotation in phase space caused by the polarizers with phase space variables given in Eq. (A25) of the Appendix.

2. Four-mode pure squeezed vacuum state

Now we consider different Gaussian states and analyze them using the framework developed above. We first analyze the nonlocality in the four-mode pure squeezed vacuum state, which corresponds to $\kappa = 1$ in Eq. (15). Figure 3 shows a plot of $f(\theta_1, \theta_2, \theta'_1, \theta'_2)$ as a function of squeezing parameter u for two different cases $v = -u$ and $v = 0$. A thick solid line represents the case $v = -u$ and it violates the CV-CH Bell-type inequality. The corresponding input state takes a very simple form $|\text{TMSV}\rangle_{13}|\text{TMSV}\rangle_{24}$ in this case, where TMSV denotes the two-mode squeezed vacuum state. The dashed line represents the case $v = 0$ and it violates the inequality indicating that the state is nonlocal. The state corresponding to the case $v = -u$ has the same entanglement structure as state $|\psi_2\rangle$ which we analyzed in Sec. III A. The values of parameters $\theta_1, \theta_2, \theta'_1,$ and θ'_2 are chosen such that the violation of the inequality is maximum.

3. Four-mode squeezed thermal state

Thermal states of the electromagnetic field arise when radiation is in contact with a thermal bath at a given temperature. We can imagine the mode under consideration to be a classical mixture of different energy states (states with different numbers of photons) with weight factors given by the Boltzmann distribution. Given a thermal source like the Sun, if we filter out a beam along a given direction and a fixed frequency, we will get thermal light for the two polarization modes. Thermal states are classical in the quantum-optical sense and the corresponding Wigner distribution is Gaussian. Thermal states when subjected to squeezing transformations lead to squeezed thermal states which again are within the class of Gaussian states however, they are nonclassical [62].

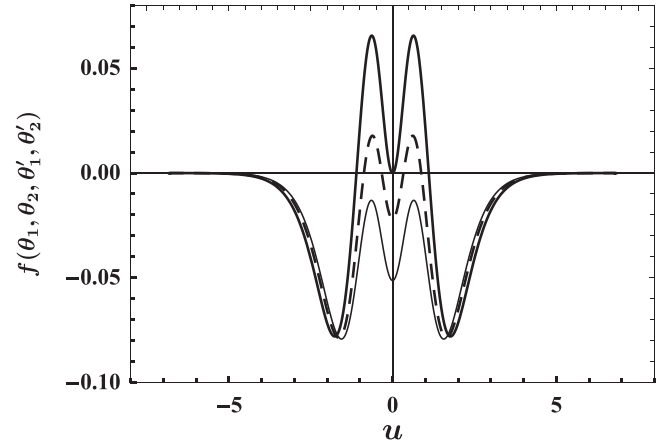


FIG. 4. Average of the Bell operator as a function of squeezing parameter u for the four-mode squeezed thermal state for the case $v = -u$. Different angles are fixed as $\theta_1 = 1.32$, $\theta_2 = 0.93$, $\theta'_1 = 3.66$, $\theta'_2 = 3.32$. Thick solid, dashed, and thin solid graphs depict $\kappa = 1$, $\kappa = 0.8$, and $\kappa = 0.7$, respectively. Results show that an increase in temperature results in loss of nonlocal correlations.

We consider four-mode squeezed thermal states for the case $v = -u$. Figure 4 shows plot of $f(\theta_1, \theta_2, \theta'_1, \theta'_2)$ as a function of squeezing parameter u for different values of κ . From this figure, it is clear that nonlocal correlations are present in the state even at a finite temperature. As the temperature increases, the detected nonlocal correlations vanish. It is also to be noted that these states are nonclassical mixed states. Similar studies have been carried out in Ref. [63], where a pure nonclassical state is mixed with a thermal state via a beam splitter and the entanglement vanishes at a certain temperature. A related phenomena termed as sudden death of entanglement, where entanglement vanishes at a finite time, is also observed in a quantum system evolving in a dissipative environment [64].

4. Leakage model

We consider a scenario in which there is leakage in the system leading to information loss and energy dissipation. Such leakages become quite important in various quantum information protocols [65], for instance, continuous-variable quantum key distribution [66], and therefore it is important to analyze the effects of such leakage processes on the state properties. Typically such leakages occur due to dissipative processes and can be modeled with beam splitters as shown in Fig. 5, where we couple each mode of the system in the state $|\Psi\rangle = |\text{TMSV}\rangle_{13}|\text{TMSV}\rangle_{24}$ with vacuum via two beam splitters of transmittance T . Subsequently, the mode corresponding to the vacuum is traced out and the output state of the system modes becomes a mixed Gaussian state. The results are shown in Fig. 6. The thick solid, dashed, and thin solid lines correspond to transmittance $T = 1, 0.8,$ and 0.6 , respectively. We observe that although there is a loss in the detected nonlocal correlations as transmittance decreases, however, it never vanishes even for low transmittance. Hence, nonlocality of the squeezed Gaussian state is preserved under leakage. This is contrary to the thermal states where detected

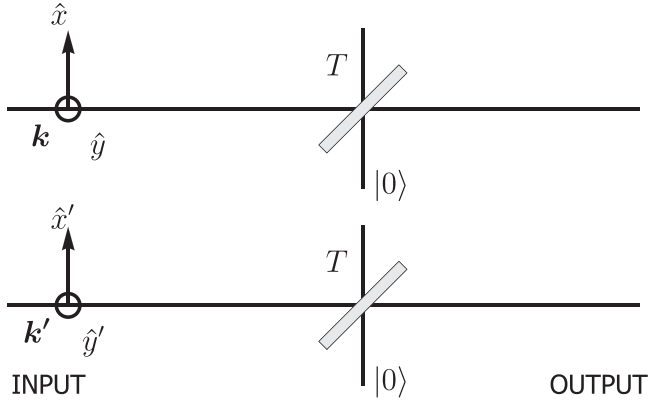


FIG. 5. Modeling leakage with beam splitters. The input state of the system is $|\text{TMSV}\rangle_{13}|\text{TMSV}\rangle_{24}$, which maximally violates the CV-CH Bell-type inequality. Each mode of the pure input state is mixed with vacuum using two beam splitters of transmittance T . Subsequently, mode corresponding to vacuum is discarded, and thus the output is a mixed state.

nonlocality completely vanishes after a certain threshold temperature.

This leakage scenario modeled by beam splitters also can be used to predict the result of a real photodetector with nonunit quantum efficiency η . A real photodetector without dark counts can be modeled as an ideal photodetector (unit quantum efficiency) preceded by a beam splitter of transmissivity η [67]. Hence, our leakage model also allows us to surmise the effects of nonunit quantum efficiency detectors without dark counts. However, a more detailed analysis will be required to model the nonunit quantum efficiency detectors with dark counts [68].

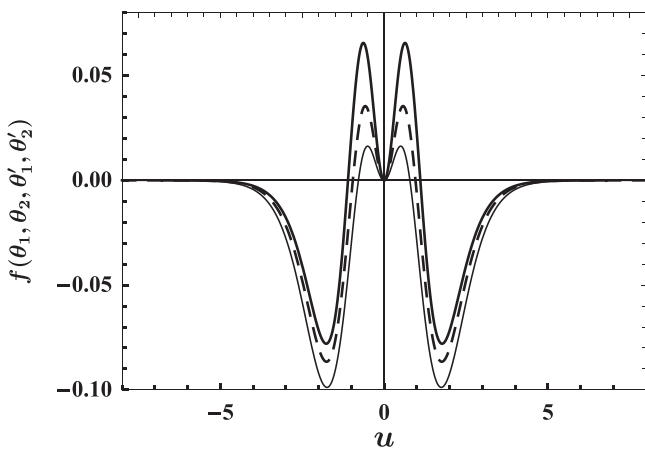


FIG. 6. Average of Bell operator as a function of squeezing parameter u for a four-mode pure squeezed vacuum state $|\text{TMSV}\rangle_{13}|\text{TMSV}\rangle_{24}$ in the presence of leakage. Different angles are fixed as $\theta_1 = 1.32$, $\theta_2 = 0.93$, $\theta'_1 = 3.66$, $\theta'_2 = 3.32$. Thick solid, dashed, and thin solid lines correspond to transmittance, $T = 1, 0.8$, and 0.6 , respectively. Results indicate that the nonlocal character of state remains preserved under leakage.

C. Non-Gaussian states

In this section, we analyze nonlocality in families of non-Gaussian states namely pair coherent states and entangled coherent states.

1. Pair coherent states

Pair coherent states, are a family of non-Gaussian entangled states of a two-mode radiation field defined as [69]

$$\hat{a}_1 \hat{a}_2 |\zeta, q\rangle = \zeta |\zeta, q\rangle, \quad (\hat{a}_1 \hat{a}_1^\dagger - \hat{a}_2 \hat{a}_2^\dagger) |\zeta, q\rangle = q |\zeta, q\rangle. \quad (20)$$

Here eigenvalue q is the photon number difference between the two modes and eigenvalue ζ is in general complex. Pair coherent states are simultaneous eigenkets of $\hat{a}_1 \hat{a}_2$ and $\hat{a}_1 \hat{a}_1^\dagger - \hat{a}_2 \hat{a}_2^\dagger$. The solution to this eigenvalue problem for positive q in the Fock basis is

$$|\zeta, q\rangle = A_q \sum_{n=0}^{\infty} \frac{\zeta^n}{[n!(n+q)!]^{1/2}} |n+q, n\rangle, \quad (21)$$

with

$$A_q = [|\zeta|^{-q} J_q(2|\zeta|)]^{-1/2}, \quad (22)$$

where J_q is the modified Bessel function of the first kind of order q . Entanglement, nonclassicality, and squeezing have been studied in pair coherent states [70–72] and these states can also be used as a resource for teleportation [73]. The covariance matrix of pair coherent states turns out to be

$$V(\zeta, q) = \begin{pmatrix} N_1 + \frac{1}{2} & \text{Re}\zeta & 0 & \text{Im}\zeta \\ \text{Re}\zeta & N_2 + \frac{1}{2} & \text{Im}\zeta & 0 \\ 0 & \text{Im}\zeta & N_1 + \frac{1}{2} & -\text{Re}\zeta \\ \text{Im}\zeta & 0 & -\text{Re}\zeta & N_2 + \frac{1}{2} \end{pmatrix}, \quad (23)$$

where $N_1 = \langle \hat{a}_1^\dagger \hat{a}_1 \rangle$ and $N_2 = \langle \hat{a}_2^\dagger \hat{a}_2 \rangle$. For non-Gaussian states, the covariance matrix does not capture the full information, nevertheless, studies have shown [70] that entanglement can be detected in pair coherent state by inequalities based on the second-order correlation. However, for nonlocality measurement, we cannot restrict to Gaussian approximation of the state via the covariance matrix. We evaluate the average of the Bell operator (16), valid for general radiation states, to determine whether the state is nonlocal or not. The Wigner function for the pair coherent states [74] can be used to calculate the required correlation functions in phase space using Eq. (18a).

We take the input state to be $|\text{PCS}\rangle_{13}|\text{PCS}\rangle_{24}$ with $q = 0$ and $\text{Im}(\zeta) = 0$, and calculate the average of the Bell operator (16). The numerically calculated average is plotted in Fig. 7 which clearly shows that the family of pair coherent states violates CV-CH Bell-type inequality.

2. Entangled coherent state

We consider the entangled coherent state (ECS) for the two-mode system as defined in Ref. [75]:

$$|\text{ECS}\rangle = N_o \left(\left| \frac{-\alpha}{\sqrt{2}} \right\rangle \left| \frac{\alpha}{\sqrt{2}} \right\rangle - \left| \frac{\alpha}{\sqrt{2}} \right\rangle \left| \frac{-\alpha}{\sqrt{2}} \right\rangle \right), \quad (24)$$

where $N_o = [2 - 2 \exp(-2|\alpha|^2)]^{-1/2}$.

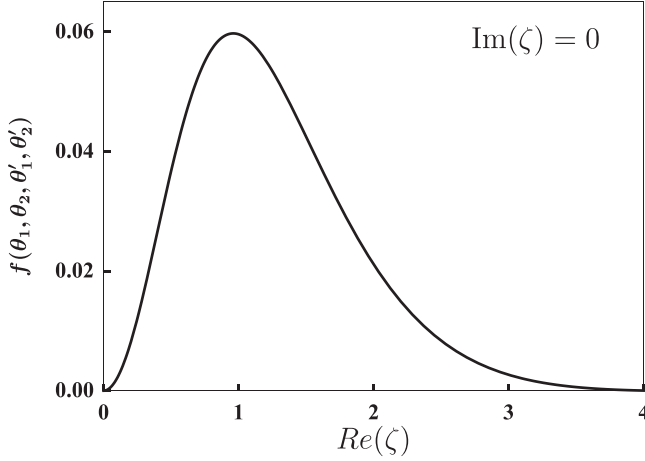


FIG. 7. Average of Bell operator as a function of parameter $\text{Re}(\zeta)$ for the pair coherent state with $q = 0$. The angles are optimized to obtain maximum violation. The result shows that the pair coherent state violates CV-CH Bell-type inequality.

We consider modes 1 and 2 (direction \mathbf{k}) initialized to vacuum state and modes 3 and 4 (direction \mathbf{k}') prepared in the odd coherent state $|\psi_o\rangle = N_o(|\alpha\rangle - |-\alpha\rangle)$. We then apply the compact passive transformation given in Eq. (3) with

$$C = -S = (1/\sqrt{2})\mathbb{1}_2, \quad U_1 = U_2 = V_1 = V_2 = \mathbb{1}_2. \quad (25)$$

This transformation corresponds to mixing of the pair of modes 1 and 2 with the pair of modes 3 and 4 using a balanced beam splitter. The final state is $|\text{ECS}\rangle_{13}|\text{ECS}\rangle_{24}$ given by

$$\begin{aligned} & N_o^2 |0\rangle_1 |0\rangle_2 (|\alpha\rangle - |-\alpha\rangle)_3 (|\alpha\rangle - |-\alpha\rangle)_4 \\ & \xrightarrow{U(D)} N_o^2 \left(\left| \frac{-\alpha}{\sqrt{2}} \right\rangle \left| \frac{\alpha}{\sqrt{2}} \right\rangle - \left| \frac{\alpha}{\sqrt{2}} \right\rangle \left| \frac{-\alpha}{\sqrt{2}} \right\rangle \right)_{13} \\ & \times \left(\left| \frac{-\alpha}{\sqrt{2}} \right\rangle \left| \frac{\alpha}{\sqrt{2}} \right\rangle - \left| \frac{\alpha}{\sqrt{2}} \right\rangle \left| \frac{-\alpha}{\sqrt{2}} \right\rangle \right)_{24}. \end{aligned} \quad (26)$$

We use Eq. (A25) given in Appendix A to compute the Wigner function of the state $N_o^2 |0\rangle_1 |0\rangle_2 (|\alpha\rangle - |-\alpha\rangle)_3 (|\alpha\rangle - |-\alpha\rangle)_4$ and then transform the Wigner function as $W(\xi) \rightarrow W(E^{-1}\xi)$ to obtain the Wigner function of the final state in Eq. (26), where E can be written as follows using Eq. (A11) given in the Appendix.

$$E = \frac{1}{\sqrt{2}} \begin{pmatrix} q_1 & q_2 & q_3 & q_4 & p_1 & p_2 & p_3 & p_4 \\ \hline 1 & 0 & -1 & 0 & 0 & 0 & 0 & 0 \\ 0 & 1 & 0 & -1 & 0 & 0 & 0 & 0 \\ 1 & 0 & 1 & 0 & 0 & 0 & 0 & 0 \\ 0 & 1 & 0 & 1 & 0 & 0 & 0 & 0 \\ \hline 0 & 0 & 0 & 0 & 1 & 0 & -1 & 0 \\ 0 & 0 & 0 & 0 & 0 & 1 & 0 & -1 \\ 0 & 0 & 0 & 0 & 1 & 0 & 1 & 0 \\ 0 & 0 & 0 & 0 & 0 & 1 & 0 & 1 \end{pmatrix} \begin{matrix} q_1 \\ q_2 \\ q_3 \\ q_4 \\ p_1 \\ p_2 \\ p_3 \\ p_4 \end{matrix} \quad (27)$$

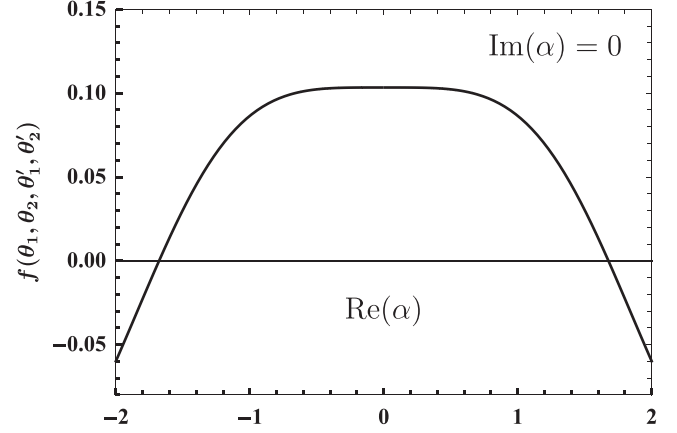


FIG. 8. Average of Bell operator as a function of $\text{Re}(\alpha)$ for the entangled coherent state. Different angles are fixed as $\theta_1 = 2.67$, $\theta_2 = 5.59$, $\theta'_1 = 1.88$, $\theta'_2 = 3.24$. The results clearly indicate that the entangled coherent state violates CV-CH Bell-type inequality.

This Wigner function can be used to compute the Bell operator in phase space; for example, Eq. (18a) evaluates to

$$\begin{aligned} \text{Tr}(\rho|0\rangle_{\theta_1, \theta_2} \langle 0|) &= 2 \frac{e^{d^2}}{(e^{d^2} - 1)^2} \left[-\cosh\left(\frac{1}{4}d^2 \cos(2\theta_1)\right) \right. \\ & \left. + \cosh\left(\frac{3}{4}d^2\right) \cosh\left(\frac{1}{4}d^2 \sin(2\theta_1)\right) \right], \end{aligned} \quad (28)$$

where $d = \text{Re}(\alpha)$ and $\text{Im}(\alpha) = 0$. The result is shown in Fig. 8 clearly indicating the violation of the CV-CH Bell-type inequality.

In the limit of $|\alpha| \rightarrow 0$, after expanding both sides of Eq. (26) in the Fock basis, we obtain

$$|0\rangle_1 |0\rangle_2 |1\rangle_3 |1\rangle_4 \xrightarrow{U(D)} \frac{1}{2} (|01\rangle - |10\rangle)_{13} (|01\rangle - |10\rangle)_{24}. \quad (29)$$

This is exactly the state $|\psi_2\rangle$ considered in Sec. (III A), which has been shown to violate the CV-CH Bell-type inequality.

D. Comparison with other Bell's inequalities

In this section, we compare the results of our CV-CH Bell inequality with three other Bell-type inequalities. We first consider the Bell-CHSH inequality based on displaced parity operator measurements [34]. The displaced parity operator acting on a two-mode system labeled by “a” and “b” is given by

$$\hat{\Pi}_{ab} = \hat{D}_a(\alpha) \hat{D}_b(\beta) (-1)^{\hat{n}_a + \hat{n}_b} \hat{D}_a(\alpha)^\dagger \hat{D}_b(\beta)^\dagger. \quad (30)$$

Using the above displaced parity operator, the average of the Bell operator can be written as [42]

$$\begin{aligned} \langle \hat{B}_{\text{CHSH}}^{\text{BW}} \rangle &= \langle \hat{\Pi}_{ab}(\sqrt{\alpha}, -\sqrt{\alpha}) \rangle + \langle \hat{\Pi}_{ab}(-3\sqrt{\alpha}, -\sqrt{\alpha}) \rangle \\ & \quad + \langle \hat{\Pi}_{ab}(\sqrt{\alpha}, 3\sqrt{\alpha}) \rangle - \langle \hat{\Pi}_{ab}(-3\sqrt{\alpha}, 3\sqrt{\alpha}) \rangle, \end{aligned} \quad (31)$$

which satisfies the condition $|\langle \hat{B}_{\text{CHSH}}^{\text{BW}} \rangle| \leq 2$ for any classical local theory. We plot the average of the Bell operator for

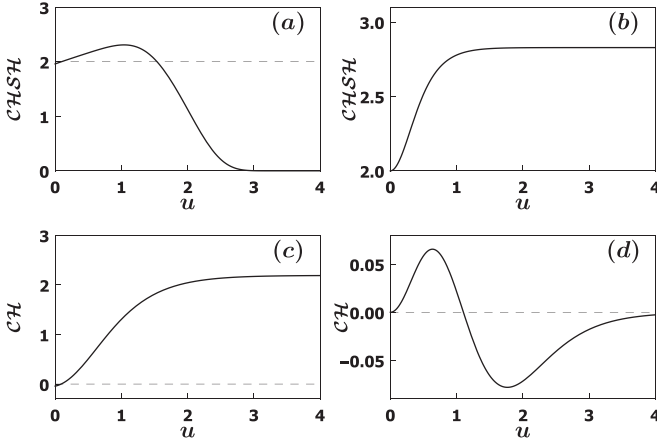


FIG. 9. Average of the Bell operator as a function of the squeezing parameter u of the TMSV state. Any quantum state violating the inequality $|\langle \mathcal{CHSH} \rangle| \leq 2$ or $-1 \leq \langle \mathcal{CH} \rangle \leq 0$ is said to be non-local. The results show that all the four Bell-type inequalities can detect nonlocality in the TMSV state. (a) Bell-CHSH inequality based on displaced parity operator measurements given by Banaszek *et al.* [34]. (b) Bell-CHSH inequality based on pseudospin measurements given by Chen *et al.* [35]. (c) CH inequality based on displaced on-off measurements given by Banaszek *et al.* [34]. (d) CH inequality based on on-off measurements given by Arvind *et al.* [33].

the TMSV state in Fig. 9(a). Here α has been optimized for maximum violation.

We next consider a Bell-CHSH inequality based on pseudospin operator measurements [35]. The pseudospin operators are defined as

$$s_z = \sum_{n=0}^{\infty} [|2n+1\rangle\langle 2n+1| - |2n\rangle\langle 2n|], \quad (32)$$

$$s_- = \sum_{n=0}^{\infty} |2n\rangle\langle 2n+1|, \quad (33)$$

$$s_+ = \sum_{n=0}^{\infty} |2n+1\rangle\langle 2n|, \quad (34)$$

where $|n\rangle$ are the usual Fock states, and s_- and s_+ are the parity flip operators. These are related to s_x and s_y as follows:

$$2s_{\pm} = s_x \pm is_y. \quad (35)$$

We define an arbitrary vector on the surface of a unit sphere as

$$\mathbf{v} = (\sin \theta \cos \phi, \sin \theta \sin \phi, \cos \theta). \quad (36)$$

Using these, the Bell-CHSH inequality is defined as

$$\begin{aligned} \langle \hat{B}_{\text{CH}}^{\text{CPHZ}} \rangle &= \langle E(\mathbf{v}_1, \mathbf{v}_2) \rangle + \langle E(\mathbf{v}_1, \mathbf{v}'_2) \rangle \\ &+ \langle E(\mathbf{v}'_1, \mathbf{v}_2) \rangle - \langle E(\mathbf{v}'_1, \mathbf{v}'_2) \rangle, \end{aligned} \quad (37)$$

where $\mathbf{v}_1, \mathbf{v}_2, \mathbf{v}'_1$, and \mathbf{v}'_2 are unit vectors, \hat{s}_1 and \hat{s}_2 are the spin operators defined using the pseudospin operators, and $E(\mathbf{v}_1, \mathbf{v}_2) = \langle (\mathbf{v}_1 \cdot \hat{s}_1) \otimes (\mathbf{v}_2 \cdot \hat{s}_2) \rangle$. For the TMSV state, we set all the azimuthal angles to be zero and choose

$$\theta_{\mathbf{v}_1} = 0, \theta_{\mathbf{v}'_1} = \pi/2, \theta_{\mathbf{v}_2} = -\theta_{\mathbf{v}'_2}, \quad (38)$$

for maximum violation. Then the average of the Bell operator becomes

$$\langle \hat{B}_{\text{CH}}^{\text{CPHZ}} \rangle = 2(\cos \theta_{\mathbf{v}_2} + K \sin \theta_{\mathbf{v}_2}), \quad (39)$$

where $\theta_{\mathbf{v}_2} = \tan^{-1} K$. The average of the Bell operator for the TMSV state is plotted in Fig. 9(b).

Finally, we consider Clauser-Horne inequality based on displaced on-off measurements [34]. The measurement operator corresponding to the displaced ‘‘on’’ measurement on individual modes is given by

$$\hat{Q}_i(\alpha) = \hat{D}_i(\alpha)|0\rangle_{ii}\langle 0|\hat{D}_i(\alpha)^\dagger, \quad (40)$$

while the measurement operator corresponding to the displaced ‘‘on’’ measurement on modes ‘‘a’’ and ‘‘b’’ is given by

$$\hat{Q}_{ab}(\alpha, \beta) = \hat{D}_a(\alpha)|0\rangle_{aa}\langle 0|\hat{D}_a(\alpha)^\dagger \otimes \hat{D}_b(\beta)|0\rangle_{bb}\langle 0|\hat{D}_b(\beta)^\dagger. \quad (41)$$

Using Clauser-Horne inequality, the corresponding CH inequality can be written as

$$\begin{aligned} \langle \hat{B}_{\text{CH}}^{\text{BW}} \rangle &= \langle \hat{Q}_{ab}(0, 0) \rangle + \langle \hat{Q}_{ab}(\alpha, 0) \rangle + \langle \hat{Q}_{ab}(0, \beta) \rangle \\ &- \langle \hat{Q}_{ab}(\alpha, \beta) \rangle - \langle \hat{Q}_a(0) \rangle - \langle \hat{Q}_b(0) \rangle, \end{aligned} \quad (42)$$

which satisfies the condition $-1 \leq \langle \hat{B}_{\text{CH}}^{\text{BW}} \rangle \leq 0$ for any classical local theory. We plot the average of the Bell operator for the TMSV state in Fig. 9(c). Here α and β have been optimized for maximum violation. We plot the average of the Bell operator for our CV-CH Bell-type inequality based on on-off measurements for the TMSV state in Fig. 9(d). The results show that all the four Bell inequalities show violation for the TMSV state.

We now discuss the experimental implementation of different Bell inequalities considered above. Since displaced parity measurements [34] and pseudospin operator measurements [35] cannot be realized with efficient homodyne detection [37], it is difficult to realize these inequalities experimentally. We next analyze the singlet state $|\psi\rangle = (|01\rangle - |10\rangle)/\sqrt{2}$ and entangled coherent state (24) using CH inequality based on displaced on-off measurements. We plot the average of the Bell operator in Fig. 10. The results show that it is necessary to perform displacement before on-off measurements to detect nonlocality of the singlet state and the entangled coherent state. To displace the state, a strong local oscillator is required. Further, to maximize the violation, we need to adjust the strength of the local oscillator, which is an arduous task [76]. In contrast, there is no such requirement of a strong local oscillator for our CV-CH Bell-type inequality. Furthermore, the maximum violation can be obtained by simply adjusting the angles of the polarizers. Therefore, our CV-CH Bell-type inequality is preferable whenever it is hard to arrange a strong local oscillator.

IV. CONCLUSION

In this work we have explored the capacity of the CV-CH Bell-type inequality to unearth the nonlocality of continuous-variable systems. In this direction, we considered a variety of states ranging from a finite number of photons to an arbitrary number of photons, Gaussian to non-Gaussian. We have used

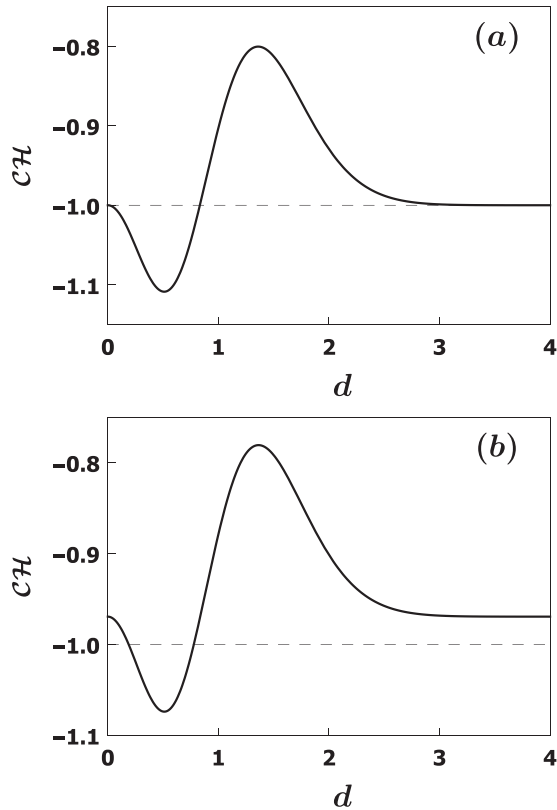


FIG. 10. Average of the Bell operator as a function of displacement “ d ” before on-off measurements. Any quantum state violating the inequality $-1 \leq \mathcal{CH} \leq 0$ is said to be nonlocal. (a) For the singlet state. (b) For the entangled coherent state.

passive transformations, which are known to convert nonclassicality into entanglement, to enhance the violation of the Bell-type inequality. The results show that the CV-CH Bell-type inequality, which is based on the Clauser-Horne 1974 Bell test inequality, is efficient in detecting nonlocality in a number of situations.

The setup for the CV-CH Bell-type inequality can accommodate four modes. The only requirement for the inequality to detect nonlocality in a given state is that the correlation should not be limited to modes 1 and 2 and modes 3 and 4 as these pairs of modes travel along the same physical directions. For mixed states, the results show that the inequality can detect nonlocality in thermal states up to a certain temperature range. On the other hand, when we consider leakage modeled by beam splitters, the violation never vanishes, although it diminishes with increasing leakage probability. We have further shown that our CV-CH inequality is preferable for the detection of violation for certain states and does not require a strong local oscillator for its implementation.

In our work, we have considered dichotomous measurements based on the presence of light or no light and coincidences thereof. We are thus using very coarse grained measurements. It would be interesting to consider coincidence count based on more fine grained measurements, where we distinguish between the different number of photons detected. Such measurements are possible now and are being used and considered in various situations [77,78]. Therefore, while the

inequality based on two outcomes is useful in unearthing the nonlocality of a variety of states, finding more general Bell-type inequalities for detecting nonlocality in CV systems is desirable. Another interesting direction we are pursuing is to generalize the CV-CH Bell-type inequality for an n -mode system.

ACKNOWLEDGMENTS

C.K. thanks Sarbani Chatterjee for encouraging discussions. A. and C.K. acknowledge financial support from DST/ICPS/QuST/Theme-1/2019/General Project No. Q-68.

APPENDIX: CONTINUOUS-VARIABLE SYSTEM: BACKGROUND MATERIAL

In this section, we briefly recapitulate the CV system and its phase space description, which have been used in our work.

1. CV system and phase space

The CV system that we consider is a four-mode system as described in Fig. 1. The annihilation operators a_j ($j = 1, 2, 3, 4$) and their conjugate creation operators can be arranged in a column vector as

$$\hat{\xi}^{(c)} = (\xi_i^{(c)}) = (\hat{a}_1, \dots, \hat{a}_4, \hat{a}_1^\dagger, \dots, \hat{a}_4^\dagger)^T, \quad i = 1, 2, \dots, 8. \quad (\text{A1})$$

The commutation relation for the field operators can be compactly written as

$$[\hat{\xi}_i^{(c)}, \hat{\xi}_j^{(c)}] = \beta_{ij}, \quad \beta = \begin{pmatrix} 0_4 & \mathbb{1}_4 \\ -\mathbb{1}_4 & 0_4 \end{pmatrix}, \quad (\text{A2})$$

where $\mathbb{1}_4$ is the 4×4 identity matrix. For the i^{th} mode, we have the corresponding state space spanned by the eigenvectors $|n_i\rangle$, with $\{n_i = 0, 1, \dots, \infty\}$ being the corresponding eigenvalues of the number operator $\hat{N}_i = \hat{a}_i^\dagger \hat{a}_i$. These eigenvectors are called Fock states or number states and the space spanned by them is the Hilbert space \mathcal{H}_i of the corresponding mode. The combined Hilbert space $\mathcal{H}^{\otimes 4} = \otimes_{i=1}^4 \mathcal{H}_i$ of the four-mode system is spanned by the product basis vector $|n_1\rangle|n_2\rangle|n_3\rangle|n_4\rangle$ with $\{n_1, n_2, n_3, n_4 = 0, 1, \dots, \infty\}$. The number n_i corresponds to photon number in the i^{th} mode. The field operators \hat{a}_i and \hat{a}_i^\dagger act irreducibly on the Hilbert space \mathcal{H}_i and their action on the number state $|n_i\rangle$ can be easily determined by the commutation relation given in Eq. (A2):

$$\begin{aligned} \hat{a}_i |n_i\rangle &= \sqrt{n_i} |n_i - 1\rangle, \quad n_i \geq 1, \quad \hat{a}_i |0\rangle = 0, \\ \hat{a}_i^\dagger |n_i\rangle &= \sqrt{n_i + 1} |n_i + 1\rangle, \quad n_i \geq 0. \end{aligned} \quad (\text{A3})$$

Alternatively, we can describe our optical setup using four pairs of Hermitian operators \hat{q}_i, \hat{p}_i for $i = 1, 2, 3, 4$ known as quadrature operators. These quadrature operators can be arranged in a column vector as

$$\hat{\xi} = (\hat{\xi}_i) = (\hat{q}_1, \dots, \hat{q}_4, \hat{p}_1, \dots, \hat{p}_4)^T, \quad i = 1, 2, \dots, 8. \quad (\text{A4})$$

The field operators and the quadrature operators are related as

$$\hat{a}_i = \frac{1}{\sqrt{2}}(\hat{q}_i + i\hat{p}_i), \quad \hat{a}_i^\dagger = \frac{1}{\sqrt{2}}(\hat{q}_i - i\hat{p}_i). \quad (\text{A5})$$

The canonical commutation relation for the quadrature operators can be written in a compact form as ($\hbar = 1$):

$$[\hat{\xi}_i, \hat{\xi}_j] = i\beta_{ij}. \quad (\text{A6})$$

The operators \hat{q}_i and \hat{p}_i satisfy the following eigenvalue equation:

$$\hat{q}_i|q_i\rangle = q_i|q_i\rangle, \quad \hat{p}_i|p_i\rangle = p_i|p_i\rangle. \quad (\text{A7})$$

The eigenvalues q_i and p_i are real and continuous and we have

$$\begin{aligned} \langle q'_i|q_i\rangle &= \delta(q'_i - q_i), & \langle p'_i|p_i\rangle &= \delta(p'_i - p_i), \\ \langle q_i|p_i\rangle &= (2\pi)^{-1/2} e^{iq_i p_i}. \end{aligned} \quad (\text{A8})$$

2. Symplectic transformations

The symplectic transformations for the four-mode system, which form the noncompact group $Sp(8, \mathcal{R})$ are the linear homogeneous transformations specified by real 8×8 matrices S and they preserve the canonical commutation relations given in Eq. (A6) while acting on the quadrature variables as

$$\hat{\xi}_i \rightarrow \hat{\xi}'_i = S_{ij} \hat{\xi}_j \quad \text{s.t.} \quad S\beta S^T = \beta. \quad (\text{A9})$$

While there are no finite dimension unitary representations of this group, according to Stone-von Neumann theorem, there exists an infinite dimensional unitary representation $\mathcal{U}(S)$, also known as the metaplectic representation, for each $S \in Sp(8, \mathcal{R})$ acting on the Hilbert space. For example, the metaplectic representation $\mathcal{U}(S)$ of S acts on the density operator as $\rho \rightarrow \mathcal{U}(S)\rho\mathcal{U}(S)^\dagger$. These unitary transformations are generated by Hamiltonians which are quadratic functions of quadrature and field operators. Further, any symplectic matrix $S \in Sp(8, \mathcal{R})$ can be decomposed as

$$S = S(X, Y)P, \quad (\text{A10})$$

where $S(X, Y)$ is the maximal compact subgroup of $Sp(8, \mathcal{R})$ isomorphic to $U(4)$ (unitary group in four dimensions) and is defined as

$$S(X, Y) = \begin{pmatrix} X & Y \\ -Y & X \end{pmatrix}, \quad X - iY \in U(4), \quad (\text{A11})$$

and $P \in \Pi(4)$ is a subset of $Sp(8, \mathcal{R})$ defined as

$$\Pi(4) = \{S \in Sp(8, \mathcal{R}) | S^T = S, S > 0\}. \quad (\text{A12})$$

In the quantum-optical context, the $U(4)$ part is referred to as passive transformation and the action of its elements in the Hilbert space through the metaplectic representation conserves the total photon number. Phase changes coupled with mixing via combinations of half- and quarter-wave plates and beam splitters can be used to generate all such transformations and are termed as passive operations. Under these transformations, the classical or nonclassical status of states does not change. However, such transformations have the potential to convert separable nonclassical states into entangled nonclassical states. On the other hand, elements of $\Pi(4)$ while acting via the metaplectic representation do not conserve the total photon number and are active transformations; they are

also called squeezing transformations as they can be used to generate squeezed states. These operations can generate nonclassicality as they can transform a classical state to a nonclassical one.

The symplectic matrix for phase shift operation acting on the quadrature operators \hat{q}_i, \hat{p}_i is given by

$$R_i(\phi) = \begin{pmatrix} \cos \phi & \sin \phi \\ -\sin \phi & \cos \phi \end{pmatrix}. \quad (\text{A13})$$

This transformation corresponds to the $U(1)$ subgroup of $Sp(2, \mathcal{R})$. This operation can be generated by Hamiltonian of the form $H = \hat{a}_i^\dagger \hat{a}_i$ and the corresponding metaplectic representation is

$$\mathcal{U}(R_i(\phi)) = \exp(-i\phi \underbrace{\hat{a}_i^\dagger \hat{a}_i}_{\text{Quadratic}}). \quad (\text{A14})$$

The symplectic matrix for a single-mode squeezing operator acting on quadrature operators (\hat{q}_i, \hat{p}_i) is written as

$$S_i(u) = \begin{pmatrix} e^{-u} & 0 \\ 0 & e^u \end{pmatrix}. \quad (\text{A15})$$

The corresponding unitary operator acting on the Hilbert space is given by

$$\mathcal{U}(S_i(u)) = \exp\left[u \underbrace{(\hat{a}_i^2 - \hat{a}_i^{\dagger 2})/2}_{\text{Quadratic}}\right]. \quad (\text{A16})$$

For two-mode systems, beam splitter transformation $B_{ij}(\theta)$ acting on quadrature operators $\hat{\xi} = (\hat{q}_i, \hat{q}_j, \hat{p}_i, \hat{p}_j)^T$ can be expressed as

$$B_{ij}(\theta) = \begin{pmatrix} \cos \theta & -\sin \theta & 0 & 0 \\ \sin \theta & \cos \theta & 0 & 0 \\ 0 & 0 & \cos \theta & -\sin \theta \\ 0 & 0 & \sin \theta & \cos \theta \end{pmatrix}. \quad (\text{A17})$$

The beam splitter transformation acting on field operators is an element of the $U(2)$ compact group.

$$\begin{pmatrix} \hat{a}_i \\ \hat{a}_j \end{pmatrix} \rightarrow \begin{pmatrix} \cos \theta & -\sin \theta \\ \sin \theta & \cos \theta \end{pmatrix} \begin{pmatrix} \hat{a}_i \\ \hat{a}_j \end{pmatrix}. \quad (\text{A18})$$

The corresponding unitary transformation for the beam splitter action is

$$\mathcal{U}(B_{ij}(\theta)) = \exp\left[\theta \underbrace{(\hat{a}_i \hat{a}_j^\dagger - \hat{a}_i^\dagger \hat{a}_j)}_{\text{Quadratic}}\right]. \quad (\text{A19})$$

The quadratic expressions involved in Eqs. (A14) and (A19) is photon number conserving, while the quadratic expression involved in Eq. (A16) is not photon conserving. The transmittance T of the beam splitter is related to θ via the relation $T = \cos^2 \theta$. For a 50-50 (balanced) beam splitter, $\theta = \pi/4$.

Our system comprises two spatial modes and each spatial mode consists of two orthogonal polarizations, and since the beam splitter acts only on distinct spatial modes, we also need to consider wave plates, which are also compact passive transformations, and can act on two distinct polarization modes. These wave plates along with beam splitters and phase shifters enable us to apply arbitrary 4×4 compact unitary transformation on any given state. The action of the half-wave plate, whose slow axis is at an angle ϕ to the transverse direction

of the electric field, on the annihilation operators $(\hat{a}_i, \hat{a}_j)^T$ is given by [79]

$$Q(\phi) = \nu(\phi)C(\pi/2)\nu(\phi)^{-1}, \quad (\text{A20})$$

with

$$\nu(\phi) = \begin{pmatrix} \cos \phi & -\sin \phi \\ \sin \phi & \cos \phi \end{pmatrix}, \quad C(\eta) = \begin{pmatrix} e^{i\eta/2} & 0 \\ 0 & e^{-i\eta/2} \end{pmatrix}. \quad (\text{A21})$$

Similarly, the action of the quarter-wave plate, whose slow axis is at an angle ϕ to the transverse direction of the electric field, on the annihilation operators (\hat{a}_i, \hat{a}_j) is given by

$$Q(\phi) = \nu(\phi)C(\pi)\nu(\phi)^{-1}. \quad (\text{A22})$$

We note that any SU(2) compact transformations can be obtained as a combination of quarter- and half-wave plates. Further, an arbitrary 4×4 compact unitary transformation can be decomposed as the following using cosine-sine decomposition [80]:

$$U = \begin{pmatrix} U_1 & 0 \\ 0 & U_2 \end{pmatrix} \underbrace{\begin{pmatrix} C & S \\ -S & C \end{pmatrix}}_D \begin{pmatrix} V_1^T & 0 \\ 0 & V_2^T \end{pmatrix}, \quad (\text{A23})$$

where U_1, U_2, V_1 , and V_2 represent 2×2 unitary transformations that can be generated by combinations of wave plates and phase shifter, while matrix D , with

$$C = \begin{pmatrix} \cos \theta_1 & 0 \\ 0 & \cos \theta_2 \end{pmatrix}, \quad S = \begin{pmatrix} \sin \theta_1 & 0 \\ 0 & \sin \theta_2 \end{pmatrix}, \quad (\text{A24})$$

can be generated using beam splitters and wave plates [81].

3. Phase space description

The Wigner distribution corresponding to a density operator $\hat{\rho}$ of a four-mode quantum system is defined as

$$W(\xi) = (2\pi)^{-4} \int d^4 q' \left\langle \mathbf{q} - \frac{1}{2}\mathbf{q}' | \hat{\rho} | \mathbf{q} + \frac{1}{2}\mathbf{q}' \right\rangle \exp(i\mathbf{q}' \cdot \mathbf{p}), \quad (\text{A25})$$

where $\mathbf{q} = (q_1, q_2, q_3, q_4)^T$, $\mathbf{p} = (p_1, p_2, p_3, p_4)^T$, and $\xi = (q_1, \dots, q_4, p_1, \dots, p_4)^T$. Thus, $W(\xi)$ is a function of eight real phase space variables for a four-mode quantum system.

First-order moments are given by

$$\langle \hat{\xi} \rangle = \text{Tr}[\hat{\rho}\hat{\xi}], \quad (\text{A26})$$

which can be changed without affecting the quantum correlations of the state by applying a displacement operator for the appropriate mode given by $D(\alpha) = e^{\alpha\hat{a}_i^\dagger - \alpha^*\hat{a}_i}$.

The second-order moments are best represented by the covariance matrix defined as

$$V = (V_{ij}) = \frac{1}{2} \langle \{\Delta\hat{\xi}_i, \Delta\hat{\xi}_j\} \rangle, \quad (\text{A27})$$

where $\Delta\hat{\xi}_i = \hat{\xi}_i - \langle \hat{\xi}_i \rangle$, and $\{, \}$ denotes an anticommutator. We note that the covariance matrix is an 8×8 real, symmetric matrix. The uncertainty principle in terms of the covariance matrix reads $V + \frac{i}{2}\beta \geq 0$, which implies that the covariance matrix is positive definite, i.e., $V > 0$.

States whose Wigner distributions are Gaussian are known as Gaussian states. Gaussian states are completely determined by their first- and second-order moments. We take the first-order moments to be zero and thus the covariance matrix determines the state. The Wigner distribution Eq. (A25) of a general zero-centered four-mode Gaussian state takes a simple form [62]:

$$W(q, p) = \pi^{-4} \sqrt{\text{Det}(G)} \exp(-\xi^T G \xi), \quad (\text{A28})$$

where G is also a real symmetric positive definite 8×8 matrix related to the covariance matrix V as $G = \frac{1}{2}V^{-1}$. First-order moments can always be put back if needed, by an appropriate phase space displacement. Coherent states, squeezed states, and thermal states are all examples of Gaussian states and the family contains entangled as well as nonentangled states.

Inner product of operators $\hat{\rho}_1$ and $\hat{\rho}_2$ can be computed in phase space and for a single-mode system is given as

$$\text{Tr}[\hat{\rho}_1 \hat{\rho}_2] = 2\pi \int_{\mathcal{R}^2} dq dp W_{\hat{\rho}_1}(q, p) W_{\hat{\rho}_2}(q, p). \quad (\text{A29})$$

4. Quantum-optical nonclassicality

From a quantum-optical point of view, the nonclassicality of quantum states is defined through the Glauber-Sudarshan representation. Arbitrary four-mode quantum states can be represented by the diagonal coherent state distribution function $\phi(\mathbf{z})$ given by

$$\hat{\rho} = \frac{1}{\pi^4} \int d^8 \mathbf{z} \phi(\mathbf{z}) |\mathbf{z}\rangle \langle \mathbf{z}|. \quad (\text{A30})$$

If the function $\phi(\mathbf{z})$ is positive and no more singular than a delta function, the state is defined to be classical, otherwise it is defined as nonclassical. Coherent states and thermal states are examples of quantum states that are classical in the above sense, whereas quantum states such as number states, squeezed states, and superposition of coherent states are all nonclassical.

To conclude, we would like to emphasize that all the discussions in the above section can be generalized for an arbitrary number of modes and details and mathematical background is available in [62,82,83].

[1] A. Einstein, B. Podolsky, and N. Rosen, *Phys. Rev.* **47**, 777 (1935).

[2] J. S. Bell, *Physics* **1**, 195 (1964).

[3] M. A. Nielsen and I. L. Chuang, *Quantum Computation and Quantum Information: 10th Anniversary Edition* (Cambridge University Press, Cambridge, 2010).

- [4] R. Horodecki, P. Horodecki, M. Horodecki, and K. Horodecki, *Rev. Mod. Phys.* **81**, 865 (2009).
- [5] N. Brunner, D. Cavalcanti, S. Pironio, V. Scarani, and S. Wehner, *Rev. Mod. Phys.* **86**, 419 (2014).
- [6] L. Masanes, Y.-C. Liang, and A. C. Doherty, *Phys. Rev. Lett.* **100**, 090403 (2008).
- [7] M. Navascués and T. Vértesi, *Phys. Rev. Lett.* **106**, 060403 (2011).
- [8] F. Buscemi, *Phys. Rev. Lett.* **108**, 200401 (2012).
- [9] E. Karimi and R. W. Boyd, *Science* **350**, 1172 (2015).
- [10] X. Song, Y. Sun, P. Li, H. Qin, and X. Zhang, *Sci. Rep.* **5**, 14113 (2015).
- [11] A. M. Steinberg, *Found. Phys.* **28**, 385 (1998).
- [12] P. Chowdhury, A. S. Majumdar, and G. S. Agarwal, *Phys. Rev. A* **88**, 013830 (2013).
- [13] S. Prabhakar, S. G. Reddy, A. Aadhi, C. Perumangatt, G. K. Samanta, and R. P. Singh, *Phys. Rev. A* **92**, 023822 (2015).
- [14] A. Aiello, F. Töppel, C. Marquardt, E. Giacobino, and G. Leuchs, *New J. Phys.* **17**, 043024 (2015).
- [15] N. Sandeau, H. Akhouchy, A. Matzkin, and T. Durt, *Phys. Rev. A* **93**, 053829 (2016).
- [16] C. H. Bennett, D. P. DiVincenzo, C. A. Fuchs, T. Mor, E. Rains, P. W. Shor, J. A. Smolin, and W. K. Wootters, *Phys. Rev. A* **59**, 1070 (1999).
- [17] S. S. Bhattacharya, S. Saha, T. Guha, and M. Banik, *Phys. Rev. Research* **2**, 012068(R) (2020).
- [18] J. S. Bell and A. Aspect, *Speakable and Unsayable in Quantum Mechanics: Collected Papers on Quantum Philosophy*, 2nd ed. (Cambridge University Press, Cambridge, 2004).
- [19] J. F. Clauser, M. A. Horne, A. Shimony, and R. A. Holt, *Phys. Rev. Lett.* **23**, 880 (1969).
- [20] J. Barrett, L. Hardy, and A. Kent, *Phys. Rev. Lett.* **95**, 010503 (2005).
- [21] A. Acín, N. Brunner, N. Gisin, S. Massar, S. Pironio, and V. Scarani, *Phys. Rev. Lett.* **98**, 230501 (2007).
- [22] L. Masanes, *Phys. Rev. Lett.* **102**, 140501 (2009).
- [23] N. Gisin, G. Ribordy, W. Tittel, and H. Zbinden, *Rev. Mod. Phys.* **74**, 145 (2002).
- [24] J. Singh, K. Bharti, and Arvind, *Phys. Rev. A* **95**, 062333 (2017).
- [25] R. F. Werner, *Phys. Rev. A* **40**, 4277 (1989).
- [26] N. D. Mermin, *Phys. Rev. Lett.* **65**, 1838 (1990).
- [27] G. Svetlichny, *Phys. Rev. D* **35**, 3066 (1987).
- [28] D. Collins, N. Gisin, S. Popescu, D. Roberts, and V. Scarani, *Phys. Rev. Lett.* **88**, 170405 (2002).
- [29] J.-D. Bancal, N. Brunner, N. Gisin, and Y.-C. Liang, *Phys. Rev. Lett.* **106**, 020405 (2011).
- [30] Z. Zhao, T. Yang, Y.-A. Chen, A.-N. Zhang, M. Żukowski, and J.-W. Pan, *Phys. Rev. Lett.* **91**, 180401 (2003).
- [31] J.-D. Bancal, J. Barrett, N. Gisin, and S. Pironio, *Phys. Rev. A* **88**, 014102 (2013).
- [32] D. Klyshko, *Phys. Lett. A* **172**, 399 (1993).
- [33] Arvind and N. Mukunda, *Phys. Lett. A* **259**, 421 (1999).
- [34] K. Banaszek and K. Wódkiewicz, *Phys. Rev. Lett.* **82**, 2009 (1999).
- [35] Z.-B. Chen, J.-W. Pan, G. Hou, and Y.-D. Zhang, *Phys. Rev. Lett.* **88**, 040406 (2002).
- [36] W. Son, i. c. v. Brukner, and M. S. Kim, *Phys. Rev. Lett.* **97**, 110401 (2006).
- [37] E. G. Cavalcanti, C. J. Foster, M. D. Reid, and P. D. Drummond, *Phys. Rev. Lett.* **99**, 210405 (2007).
- [38] G. Adesso and S. Piano, *Phys. Rev. Lett.* **112**, 010401 (2014).
- [39] V. Pozsgay, F. Hirsch, C. Branciard, and N. Brunner, *Phys. Rev. A* **96**, 062128 (2017).
- [40] B. Xu, T. Tufarelli, and G. Adesso, *Phys. Rev. A* **95**, 012124 (2017).
- [41] Y. Xiang, B. Xu, L. Mišta, T. Tufarelli, Q. He, and G. Adesso, *Phys. Rev. A* **96**, 042326 (2017).
- [42] S. Olivares and M. G. A. Paris, *Phys. Rev. A* **70**, 032112 (2004).
- [43] A. Ferraro and M. G. A. Paris, *J. Opt. B: Quantum Semiclassical Opt.* **7**, 174 (2005).
- [44] H. Jeong, *Phys. Rev. A* **78**, 042101 (2008).
- [45] H.-J. Kim, J. Kim, and H. Nha, *Phys. Rev. A* **88**, 032109 (2013).
- [46] E. C. G. Sudarshan, *Phys. Rev. Lett.* **10**, 277 (1963).
- [47] R. J. Glauber, *Phys. Rev.* **131**, 2766 (1963).
- [48] A. Ferraro and M. G. A. Paris, *Phys. Rev. Lett.* **108**, 260403 (2012).
- [49] V. Chille, N. Quinn, C. Peuntinger, C. Croal, L. Mišta, C. Marquardt, G. Leuchs, and N. Korolkova, *Phys. Rev. A* **91**, 050301(R) (2015).
- [50] M. Brunelli, C. Benedetti, S. Olivares, A. Ferraro, and M. G. A. Paris, *Phys. Rev. A* **91**, 062315 (2015).
- [51] M. G. A. Paris, *Phys. Rev. A* **59**, 1615 (1999).
- [52] M. S. Kim, W. Son, V. Bužek, and P. L. Knight, *Phys. Rev. A* **65**, 032323 (2002).
- [53] J. K. Asbóth, J. Calsamiglia, and H. Ritsch, *Phys. Rev. Lett.* **94**, 173602 (2005).
- [54] J. S. Ivan, S. Chaturvedi, E. Ercolessi, G. Marmo, G. Morandi, N. Mukunda, and R. Simon, *Phys. Rev. A* **83**, 032118 (2011).
- [55] I. I. Arkhipov, J. Peřina, J. Peřina, and A. Miranowicz, *Phys. Rev. A* **94**, 013807 (2016).
- [56] H. Gholipour and F. Shahandeh, *Phys. Rev. A* **93**, 062318 (2016).
- [57] S. Fu, S. Luo, and Y. Zhang, *Europhys. Lett.* **128**, 30003 (2020).
- [58] A. Gilchrist, P. Deuar, and M. D. Reid, *Phys. Rev. Lett.* **80**, 3169 (1998).
- [59] W. J. Munro, *Phys. Rev. A* **59**, 4197 (1999).
- [60] R. García-Patrón, J. Fiurášek, N. J. Cerf, J. Wenger, R. Tualle-Brouri, and P. Grangier, *Phys. Rev. Lett.* **93**, 130409 (2004).
- [61] J. F. Clauser and M. A. Horne, *Phys. Rev. D* **10**, 526 (1974).
- [62] Arvind, B. Dutta, N. Mukunda, and R. Simon, *Pramana* **45**, 471 (1995).
- [63] R. Tahira, M. Ikram, H. Nha, and M. S. Zubairy, *Phys. Rev. A* **79**, 023816 (2009).
- [64] J. P. Paz and A. J. Roncaglia, *Phys. Rev. Lett.* **100**, 220401 (2008).
- [65] K. P. Seshadreesan, H. Krovi, and S. Guha, *Phys. Rev. A* **100**, 022315 (2019).
- [66] I. Derkach, V. C. Usenko, and R. Filip, *Phys. Rev. A* **96**, 062309 (2017).
- [67] C. Weedbrook, S. Pirandola, R. García-Patrón, N. J. Cerf, T. C. Ralph, J. H. Shapiro, and S. Lloyd, *Rev. Mod. Phys.* **84**, 621 (2012).
- [68] C. Invernizzi, S. Olivares, M. G. A. Paris, and K. Banaszek, *Phys. Rev. A* **72**, 042105 (2005).
- [69] G. S. Agarwal, *Phys. Rev. Lett.* **57**, 827 (1986).

- [70] G. S. Agarwal and A. Biswas, *J. Opt. B: Quantum Semiclassical Opt.* **7**, 350 (2005).
- [71] G. S. Agarwal, *J. Opt. Soc. Am. B* **5**, 1940 (1988).
- [72] Arvind, *Phys. Lett. A* **299**, 461 (2002).
- [73] A. Gábris and G. S. Agarwal, *Int. J. Quantum. Inform.* **05**, 17 (2007).
- [74] X.-G. Meng, J.-S. Wang, and H.-Y. Fan, *Phys. Lett. A* **363**, 12 (2007).
- [75] B. C. Sanders, *Phys. Rev. A* **45**, 6811 (1992).
- [76] K. G. Fedorov, L. Zhong, S. Pogorzalek, P. Eder, M. Fischer, J. Goetz, E. Xie, F. Wulschner, K. Inomata, T. Yamamoto, Y. Nakamura, R. Di Candia, U. Las Heras, M. Sanz, E. Solano, E. P. Menzel, F. Deppe, A. Marx, and R. Gross, *Phys. Rev. Lett.* **117**, 020502 (2016).
- [77] G. S. Thekkadath, D. S. Phillips, J. F. F. Bulmer, W. R. Clements, A. Eckstein, B. A. Bell, J. Lugani, T. A. W. Wolterink, A. Lita, S. W. Nam, T. Gerrits, C. G. Wade, and I. A. Walmsley, *Phys. Rev. A* **101**, 031801(R) (2020).
- [78] C. Kumar, R. Sengupta, and Arvind, *Phys. Rev. A* **102**, 012616 (2020).
- [79] R. Simon and N. Mukunda, *Phys. Lett. A* **143**, 165 (1990).
- [80] G. W. Stewart, *Numer. Math.* **40**, 297 (1982).
- [81] I. Dhand and S. K. Goyal, *Phys. Rev. A* **92**, 043813 (2015).
- [82] Arvind, B. Dutta, C. L. Mehta, and N. Mukunda, *Phys. Rev. A* **50**, 39 (1994).
- [83] Arvind, B. Dutta, N. Mukunda, and R. Simon, *Phys. Rev. A* **52**, 1609 (1995).